INL/CON-10-19705
PREPRINT

Study on Air Ingress Mitigation Methods in the Very High Temperature Gas Cooled Reactor (VHTR)

AJTEC 2011

Chang H. Oh
Eung S. Kim

March 2011

Proceedings of the ASME/JSME 2011 8th Thermal Engineering Joint Conference
AJTEC2011
March 13-17, 2011, Honolulu, Hawaii, USA

AJTEC2011-44417

STUDY ON AIR INGRESS MITIGATION METHODS IN THE VERY HIGH TEMPERATURE GAS COOLED REACTOR (VHTR)

Chang H. Oh
Idaho National Laboratory
Idaho Falls, ID. 83415

Eung S. Kim
Idaho National Laboratory
Idaho Falls, ID. 83415

ABSTRACT

An air-ingress accident followed by a pipe break is considered as a critical event for a very high temperature gas-cooled reactor (VHTR) safety. Following helium depressurization, it is anticipated that unless countermeasures are taken, air will enter the core through the break leading to oxidation of the in-core graphite structure. Thus, without mitigation features, this accident might lead to severe exothermic chemical reactions of graphite and oxygen depending on the accident scenario and the design. Under extreme circumstances, a loss of core structural integrity may occur along with excessive release of radiological inventory.

Idaho National Laboratory under the auspices of the U.S. Department of Energy is performing research and development (R&D) that focuses on key phenomena important during challenging scenarios that may occur in the VHTR. Phenomena Identification and Ranking Table (PIRT) studies to date have identified the air ingress event, following on the heels of a VHTR depressurization, as very important (Oh et al. 2006, Schultz et al. 2006). Consequently, the development of advanced air ingress-related models and verification and validation (V&V) requirements are part of the experimental validation plan.

This paper discusses about various air-ingress mitigation concepts applicable for the VHTRs. The study begins with identifying important factors (or phenomena) associated with the air-ingress accident using a root-cause analysis. By preventing main causes of the important events identified in the root-cause diagram, the basic air-ingress mitigation ideas can be conceptually derived. The main concepts include (1) preventing structural degradation of graphite supporters; (2) preventing local stress concentration in the supporter; (3) preventing graphite oxidation; (4) preventing air ingress; (5) preventing density gradient driven flow; (6) preventing fluid density gradient; (7) preventing fluid temperature gradient; (7) preventing high temperature. Based on the basic concepts listed above, various air-ingress mitigation methods are proposed in this study. Among them, the following one mitigation idea was extensively investigated using computational fluid dynamic codes (CFD) in terms of helium injection in the lower plenum.

The main idea of the helium injection method is to replace air in the core and the lower plenum upper part by buoyancy force. This method reduces graphite oxidation damage in the severe locations of the reactor inside. To validate this method, CFD simulations are addressed here. A simple 2-D CFD model was developed based on the GT-MHR 600MWt as a reference design. The simulation results showed that the helium replaces the air flow into the core and significantly reduces the air concentration in the core and bottom reflector potentially protecting oxidation damage. According to the simulation results, even small helium flow was sufficient to remove air in the core, mitigating the air-ingress successfully.

INTRODUCTION

Idaho National Laboratory is performing research and development that focuses on key phenomena that are important during challenging scenarios that may occur in the very high temperature reactor (VHTR). Phenomena Identification and Ranking studies to date have identified the air ingress event, following on the heels of a VHTR depressurization, as very important (Schultz et al. 2006). Consequently, the development of advanced air ingress-related models and verification and validation are of very high priority for the next generation nuclear plant (NGNP) Project.

Following a loss of coolant and system depressurization incident, air ingress will occur through the break, leading to oxidation of the in-core graphite structure and fuel. Our study indicates that depending on the location and the size of the pipe break, the air ingress phenomena are different. In an effort to estimate the proper safety margin, experimental data and tools, including accurate multidimensional thermal-hydraulic and reactor physics models, a burn-off model, and a fracture model of graphite are needed. It will also require effective strategies to mitigate the effects of oxidation. The results from this research will provide crucial inputs to the INL NGNP/VHTR Methods Research and Development project.

The air ingress mitigation method developed in this study seems very promising according to our CFD (ANSYS, 2008) calculations. The experimental test data will be valuable for validating our CFD models in the near future.

OVERVIEW OF AIR INGRESS MITIGATION CONCEPTS

A Loss-of-Coolant-Accident (LOCA), which can cause depressurized conduction cool down, is considered a critical event for a VHTR. Following helium depressurization, it is anticipated that unless countermeasures are taken, air will enter the core through the break leading to oxidation of the in-core graphite structure. Thus, without mitigation features, a LOCA will lead to an air ingress event, which may lead to exothermic chemical reactions of graphite with oxygen. Under extreme circumstances, a loss of core structural integrity may occur along with excessive release of radiological inventory. The rate of graphite oxidation and the likelihood of extensive structural damage can be assessed with a combination of analytical investigation, simulations of simplified core models, and experimental validation.

This paper discusses air ingress mitigation concepts. Some important factors affecting an air-ingress accident were first figured out using a root-cause diagram shown in Figure 1. Overall air-ingress mechanisms and their relationships were also discussed here.

Before discussing air-ingress mitigation methods, it is helpful to understand the overall sequence of the air-ingress accident. Figure 1 is a top to bottom root-cause diagram that shows the overall sequence of the air ingress accident. Figure 1 indicates that graphite structure weakening is now the most serious concern in the air-ingress accident because it can lead to the fission product release and eventually to potential core weakening. Graphite structural weakening can be generated by two main causes associated with graphite oxidation: (1) degradation of graphite structures, and (2) increases in local load (stress). The graphite structure degradation is mainly caused by internal oxidation reaction in the graphite pores. The oxidation between oxygen and graphite attacks internal graphite pore structures by weakening mechanical strength. This internal oxidation occurs at rather low temperatures where the oxidation rate is slow and is controlled by reaction kinetics regime. When the internal corrosion is dominant, only graphite density is

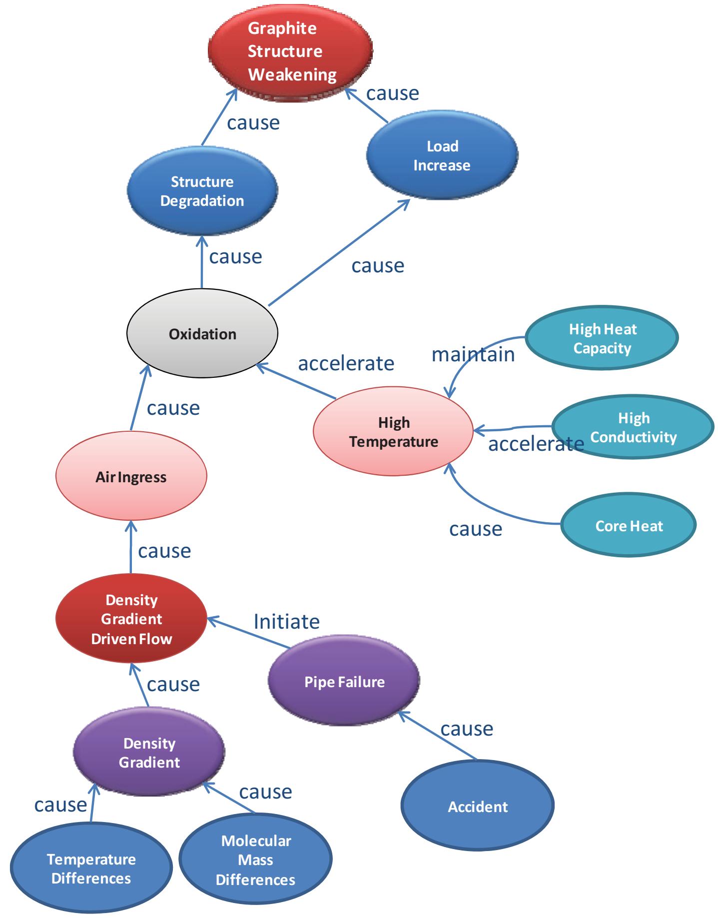

Figure 1. Root causes of Air-Ingress Accident.

decreased without external shape and size changes. Generally, the kinetics-controlled regime is the major oxidation mechanism at lower than about 650°C. On the other hand, the local stress increase is caused by external corrosion, which occurs when the oxidation rate is very fast and the process is controlled by the mass transfer of oxygen in the flow (diffusion-controlled regime). The external corrosion changes the graphite's external shape by decreasing the local supporting area. The decrease of the local supporting area concentrates the load and stress on this region. Generally, graphite oxidation is dominated by the external corrosion at higher than 950°C. At intermediate temperatures between 650 and 950°C, both internal and external corrosions are mixed together.

As shown in the middle of Figure 1, weakening of the graphite structure is caused by (1) air ingress, and (2) high temperature. The root cause of these conditions originates from the temperature and molecular mass differences between the inside and outside of the reactor vessel. Since the oxygen in the ingressed air is the main reactant, graphite oxidation does not occur without air-ingress. The oxidation rates and structural failure are greatly affected by how fast the air is ingressed. According to the Arrhenius model, the high temperature in the reactor inside significantly accelerates the graphite oxidation because the oxidation reaction exponentially increases with temperature.

The air-ingress speed is reportedly dependent on two physical mechanisms: molecular diffusion, and density gradient driven flow. However, recent studies for the double-ended-guillotine break (DEBG) showed that molecular diffusion is negligible compared to density gradient flow, since the molecular diffusion process is too slow. For this reason, molecular diffusion is removed from the diagram in Figure 1. Density gradient flow is generated in the VHTR air-ingress accident by density gradient from either molecular mass differences or temperature gradients between the inside and outside of the reactor. The initial density gradient flow is generated by molecular mass differences between helium (inside) and air (outside). However, after the air fills the bottom of the reactor vessel, the temperature gradient is the main driving force of the density gradient flow. According to this study, the density gradient flow driven by the temperature gradient is even maintained after the onset natural circulation (ONC) by accelerating air-ingress into the lower plenum one order of magnitude higher than the global natural circulation through the core.

Some basic concepts for air-ingress mitigation can be derived from removing the root causes. If the main causes of the root-cause diagram shown in Figure 1 are prevented or mitigated, the air-ingress consequences can be mitigated. The basic air-ingress mitigations are to prevent:

1. Fracture (under structural degradation or load increase conditions)
2. Structural Degradation (under oxidation environment)
3. Load Increase (under oxidation environment)
4. Oxidation (under air-ingress and high temperature conditions)
5. Air Ingress (under density gradient existing conditions)
6. Density Gradient Driven Flow (under density gradient existing conditions)
7. Density Gradient (under temperature and molecular mass difference existing conditions)
8. Temperature Gradient (between inside and outside of the reactor)
9. Molecular Mass Difference (between inside and outside of the reactor)
10. High Temperature (in the reactor inside).

PREVENTION (OR MITIGATION) OF OXIDATION BY HELIUM INJECTION INTO THE LOWER PLENUM

Since graphite oxidation is the main cause of all related air-ingress accident problems, preventing oxidation in the reactor is a very effective way to mitigate air-ingress.

The proposed method for mitigating oxidation is to inject helium into the lower plenum (See Figure 2). The main idea of this method is to inject light helium gas into the lower plenum from the lower plenum side and separate air inflow into two layers. Since the helium gas is much lighter than the air gas, the upper part of the air flow will be replaced by the helium gas, which will then move into the core channels instead of air, thus protecting the core from oxidation damage. Injecting helium into the lower plenum vessel wall of a prismatic-type reactor could also mitigate air ingress and minimize graphite oxidation by two technical reasons: (a) diluting the oxygen concentration and (b) reducing the buoyancy force by lowering fluid temperature in the lower plenum. To validate this method, a CFD simulation was performed. The simulation results showed that the helium replaces the air flow into the core and significantly reduces the air concentration in the core and bottom reflector, potentially leading to significant oxidation damages without the helium injection. According to the simulation results, even small helium flow was sufficient to remove air in the core, mitigating the air-ingress successfully.

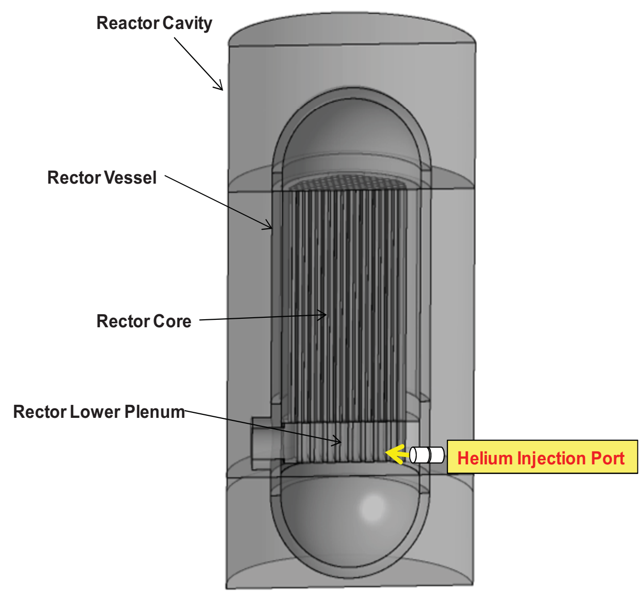

Figure 2. Air-ingress mitigation method at the lower plenum.

The second order upwind option was used for the accuracy and the computational meshes were reduced until the grid independence was established.

Figure 3 shows the geometry and the 2-D grid model for the CFD analyses. The grid model was developed by GAMBIT mesh generation software. The geometry was simplified to be 2-D for saving time in computations. The grid mode was divided into seven regions: core, lower plenum, hot-leg, cold leg, vessel inside, enclosure, and confinement. Of these regions, the core was assumed to be the porous media.

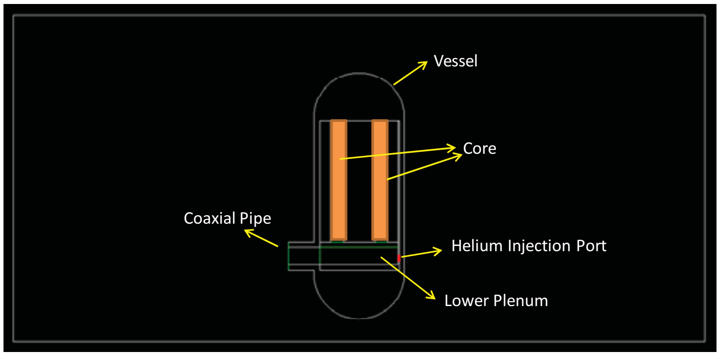

(a) Geometry summary.

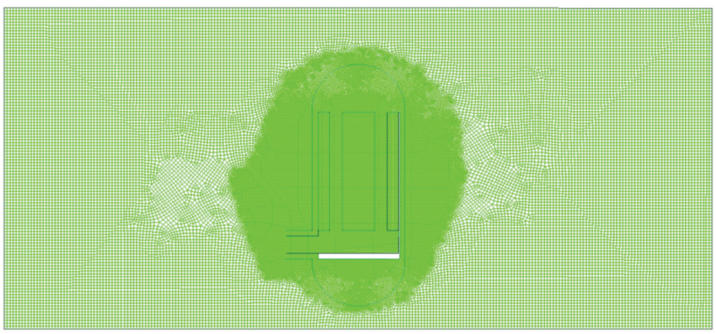

(b) Grid model (55,590 cells).

Figure 3. 2D FLUENT model (geometry and grid model).

In this analyses, the porous media are modeled by the addition of a momentum source term to the standard fluid equation. The source term is composed of two parts: a viscous loss term (Darcy, the first term), and an inertial loss term.

$$S_i = -\left(\sum_{j=1}^{3} D_{ij} \mu v_j + \sum_{j=1}^{3} C_{ij} \frac{1}{2} \rho v_{mag} v_j \right) \tag{1}$$

where S_i is the source term for the ith (x, y, or z) momentum equation, D_{ij} and C_{jj} are the viscous loss coefficient matrices and the inertia loss coefficient matrices, respectively to calculate the pressure gradient in the porous media.

To recover the case of simple homogeneous porous media

$$S_i = -\left(\frac{\mu}{\alpha} v_i + C_2 \frac{1}{2} \rho v_{mag} v_i \right) \tag{2}$$

where α is the permeability and C_2 is the inertial resistance factor, simply specify D_{ii} and C_{jj} as diagonal matrices with $1/\alpha$ and C_2, respectively, on the diagonals (and zero for the other elements). V_{mag} is the magnitude of local superficial velocity.

FLUENT also allows the source term to be modeled as a power law of the velocity magnitude:

$$S_i = -C_0 |v|^{C_1} \tag{3}$$

where C_0 and C_1 are user-defined empirical coefficients.

Two important parameters define the porous media: porosity and permeability. The process to determine these parameters for the reactor core and the lower plenum is described in the following paragraphs:

Porosity: The porosity is the volume fraction equal to the fluid volume over the total volume (where the total volume equals the fluid volume plus the structural volume) of the region in question. The porosity is used in the calculation of the heat transfer in the medium and in the time-derivative term in the scalar transport equations for unsteady flow. It also influences the calculation of the reaction source terms and body forces in the medium. These sources will be proportional to the fluid volume in the medium.

In this study, two porosities were defined: the reactor core and the lower plenum. Figure 4 shows a typical VHTR reactor core block. The porosity of the core zone is

$$\gamma_{core} = \frac{V_{fluid}}{V_{total}} = \frac{A_{fluid}}{A_{total}} = \frac{\frac{1}{8}\pi d^2}{\frac{\sqrt{3}}{4} p^2} \tag{4}$$

and the porosity of the lower plenum, based on the geometry shown in Figures 5 and 6 is

$$\gamma_{lowerplenum} = \frac{V_{fluid}}{V_{total}} = \frac{A_{fluid}}{A_{total}} = \frac{\frac{\sqrt{3}}{4} p_{LP}{}^2 - \frac{1}{8}\pi d_{LP}{}^2}{\frac{\sqrt{3}}{4} p_{LP}{}^2} \tag{5}$$

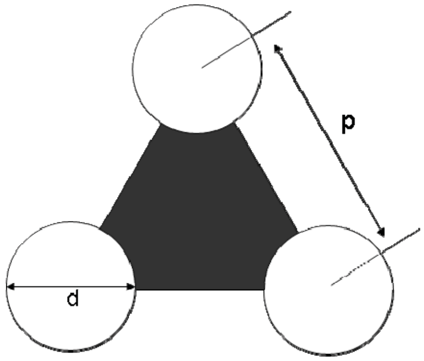

Figure 4. Core pattern (d=1.58 cm, p=3.27 cm).

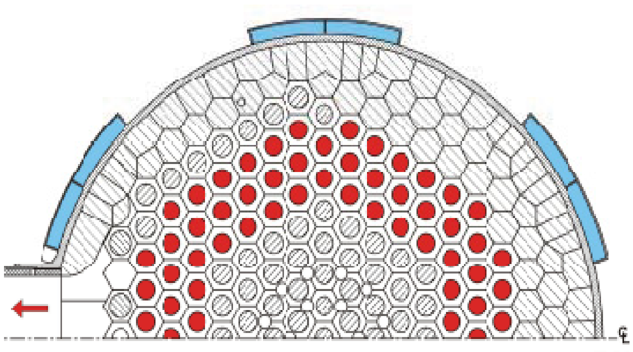

Figure 5. Typical geometry of lower plenum (d=0.212 m, p=0.36m).

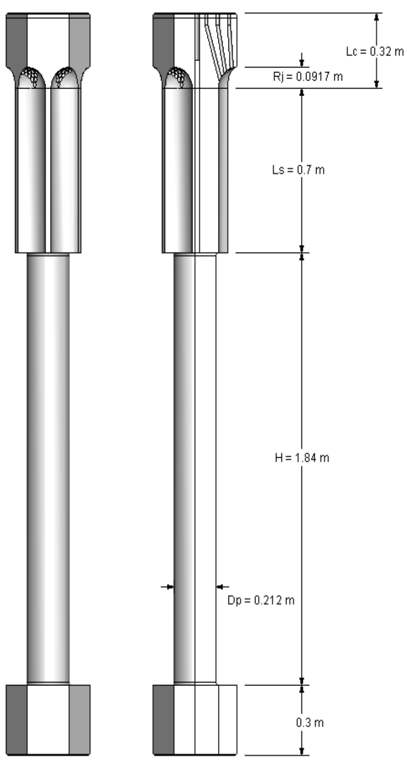

Figure 6. Detail view of lower plenum in GT-MHR 600 MWt.

From the above equations, the porosities of the reactor core and the lower plenum were calculated to be 0.21 and 0.68 respectively.

Permeability: The permeability of the porous media model is a measure of the flow conductance of the porous media. In this study the permeability was calculated in the horizontal (x-direction) and vertical (y-direction) for both the reactor core and the lower plenum. The core and the lower plenum regions were treated differently.

The stratified flow in the lower plenum will occur with very hot helium passing over confinement-temperature air. Although the stratified flow is density-driven, the density gradients will be influenced by the large temperature differences in addition to the inherent density differences that exist between helium and air. Consequently, the temperature and gas specie-driven density gradients will be large and the flow will likely be turbulent.

The flow from the lower plenum into the core will be driven by concentration-driven diffusion and the buoyancy imparted to the air by localized heating. Because these density gradients will be low, the flow will likely be laminar.

A. Reactor core: The permeability in the vertical direction was determined by adapting the relationships for circular pipe flow. Figure 7 shows the friction factor as a function of Reynolds number, as expressed in the Moody diagram for a smooth pipe, where the Reynolds number is defined in terms of pipe diameter. The pipe diameter is correlated to the porous media using hydraulic diameter for packed spheres.

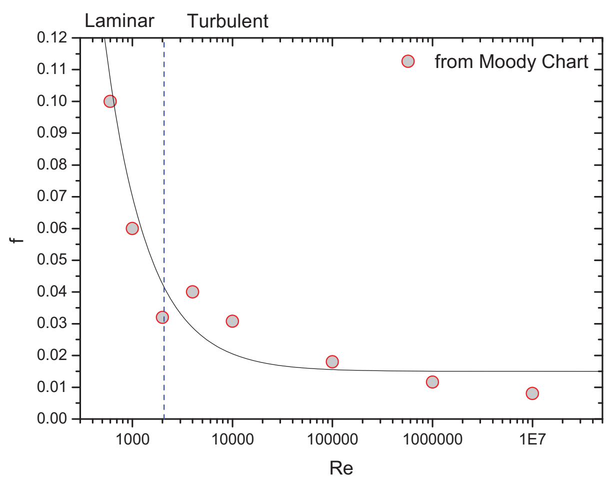

Figure 7. Friction factors as a function of Reynolds number.

To estimate the permeability and inertial resistance, a friction loss correlation (solid line) was fitted to the Moody diagram data as given by Eqn. (9).

$$f = a + \frac{b}{\mathrm{Re}} \cdot \quad (6)$$

Based on Figure 7, the friction factor equation can be correlated as follows.

$$f = 0.015 + \frac{55}{\mathrm{Re}} \cdot \quad (7)$$

The pressure drop correlation is

$$\Delta P = f\left(\frac{1}{2}\rho u^2\right)\left(\frac{L}{D}\right) \quad (8)$$

Inserting Eqn. (7) into Eqn. (8) yields

$$\Delta P = \left(0.015 + \frac{55}{\mathrm{Re}}\right)\left(\frac{1}{2}\rho u^2\right)\left(\frac{L}{D}\right) \cdot \quad (9)$$

$$\Delta P = \left(0.015 + \frac{55}{(\rho u D/\mu)}\right)\left(\frac{1}{2}\rho u^2\right)\left(\frac{L}{D}\right) \cdot \quad (10)$$

$$\frac{\Delta P}{L} = \frac{55}{2D^2}\mu u + \frac{0.015}{D}\left(\frac{1}{2}\rho u^2\right) \cdot \quad (11)$$

Therefore, the permeability (α) and inertial resistance (C_2) are

$$\alpha = \frac{2}{55} D^2, \quad (12)$$

$$C_2 = \frac{0.015}{D} \cdot \quad (13)$$

Since the channel diameter in the core is 0.0158 m, the permeability and inertial resistance are 0.00000908 m^2 and 0.949 m^{-1} respectively. The permeability and the inertia resistance in the core, x-direction can be assumed to be zero and infinite, respectively, as the horizontal flow is negligible in the reactor core.

B. Lower plenum: The porous media parameters in the vertical direction of the lower plenum were determined in the same method as the reactor core. Since the hydraulic diameter in the lower plenum is 0.46 m, the permeability and inertial resistance were calculated to be 0.00769 m^2 and 0.0326 m^{-1} respectively.

The flow resistance in the x-direction of the lower plenum must include the cross flow through the tube array. Figure 8 shows the flow and tube nomenclature.

Figure 9 shows several well known data sets for crossflow. A correlation between the friction factor and the data as a function of Reynolds number is given by the curve fit (solid line).

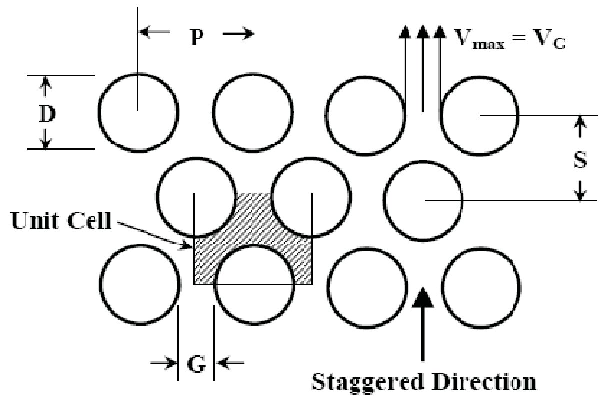

Figure 8. Equally spaced triangular tube array.

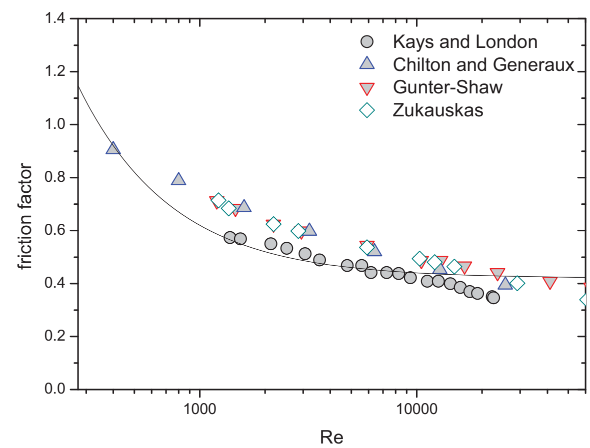

Figure 9. Cross-flow friction factor as a function of Reynolds number.

The friction factor can be correlated as shown in Eqn. (17).

$$f = 0.42 + \frac{200}{\mathrm{Re}} \quad (17)$$

which enables the pressure loss correlation to be expressed by Eqn. (18):

$$\frac{\Delta P}{L} = \frac{100}{D^2}\mu u + \frac{0.42}{D}\left(\frac{1}{2}\rho u^2\right) \cdot \quad (18)$$

Therefore, the permeability and inertial resistance are calculated as 0.002116 m^2 and 0.913 m^{-1} respectively.

The permeability of the lower plenum y-direction was determined in the same manner as the core. However, since the lower plenum geometry must consider flow moving parallel to columns, instead of within channels such as occur in the core, the lower plenum hydraulic diameter was used as the basis to estimate the permeability. The hydraulic diameter of the lower plenum (equals 0.46 m) was calculated using a standard approach based on four times the flow area divided by the wetted perimeter. Using the approach summarized above, the permeability is 0.00668 m^2.

RESULTS AND DISCUSSIONS

Figures 10, 11, and 12 show the CFD results for the three cases with different injection velocities. The selected velocities are 0.0, 0.1, and 0.5 m/s, respectively. Figure 10 shows the contour plot of the air mass fractions for no helium injection case (V_{inj} = 0.0 m/s). In this case, the air initially enters the reactor inside by the density gradient flow and is driven into the core rapidly by buoyancy force generated in the lower plenum, which is the reference case to be compared with mitigation results.

When the helium is injected at 0.1 m/s (See Figure 11), the air concentration in the core and the upper part of the lower plenum was much more reduced. When the helium is injected to the lower plenum with the speed higher than 1.0 m/s, most of air in the core and the upper lower plenum was replaced by the injected helium flow, showing clear separation of air and helium. This effect is contributed by low helium density compared to that of air. Air flow was clearly separated from the helium, and returned back to the broken hot-leg by recirculation flow. The majority of the helium injected at the lower plenum moved into the core and was released out of the vessel through the cold-leg. According to the previous air-ingress researches, the upper part of the lower plenum and the lower part of the bottom reflector are known to be the most seriously corroded and damaged by graphite oxidation because of relatively high temperature and large air concentrations. Therefore, helium injection at the lower plenum is considered to be very effective to mitigate air-ingress consequences since the injected helium successfully covers the seriously-damaged part. It indicates that the injection of helium can protect not only the core but also the lower plenum and the bottom reflectors from the serious oxidation damages. Figures 10 to 12 show the comparisons on the air distributions in the reactor for various injection speeds.

As described above, the injection fluid and the mass flow rate are very important. Based on the 200 m^3 helium storage tank with approximately 86 atm (assumption), a helium flow rate of 0.5 m/s will last 6 days; the decay heat is so after a 3 day delay by the injection that oxidation cannot be a serious problem. According to the previous investigations, the maximum temperatures of the bottom reflector and the lower plenum drop down to about 725°C and 550°C, respectively. For this idea, we propose the air velocity higher than 0.5 m/s to achieve sufficiently low air concentration in the core. The helium can be supplied from the helium supply tanks and helium storage tanks already installed in the system to maintain the pressure in the system. Depending on the helium storage tank size and injection velocity, the air-ingress delay time can be varied.

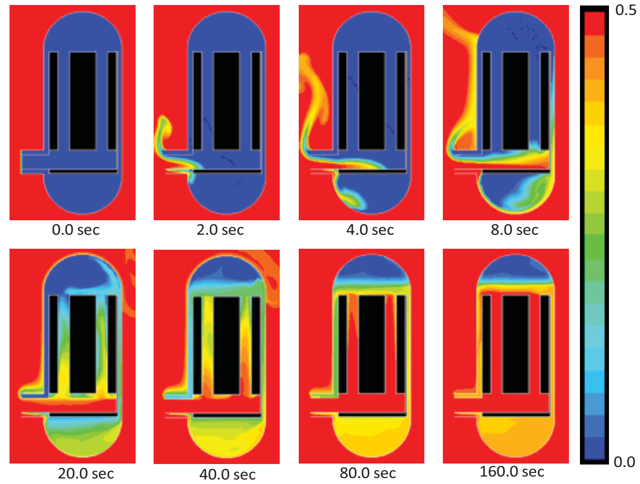

Figure 10. Helium injection (V_{inj} = 0.0 m/s).

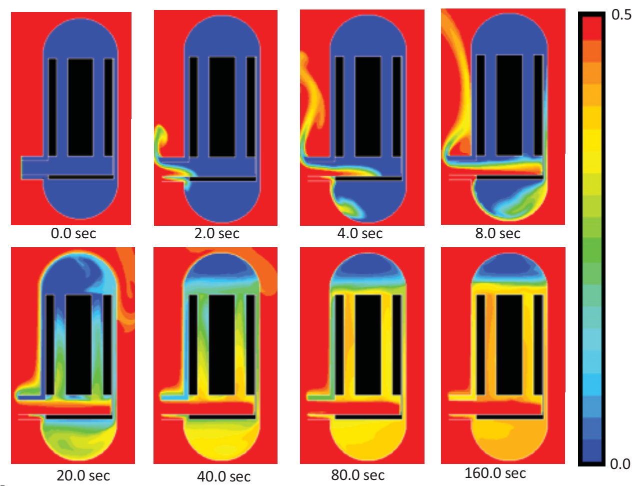

Figure 11. Helium injection (V_{inj} = 0.1 m/s).

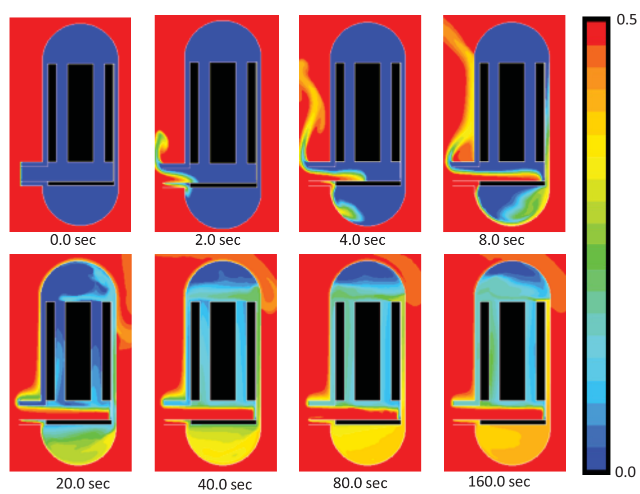

Figure 12. Helium injection (V_{inj} = 0.5 m/s).

CONCLUSIONS

Important factors affecting air-ingress consequences were investigated from root-cause analyses as a starting point of the air-ingress mitigation study. The basic air-ingress ideas were developed from this analysis.

From the basic concepts, various air-ingress mitigation methods were investigated. Among them, the following two mitigation methods were strongly recommended.

- *Helium injection in the lower plenum*. This method injects helium into the lower plenum, which replaces the air in the core and the lower plenum upper part by buoyancy force, significantly reducing graphite oxidation inside the reactor.
- *Reactor enclosure opened at the bottom*. This method encloses the reactor in a nonpressure boundary. Some design modifications of the cavity can be used for this. This enclosure has an opening at the bottom. After depressurization, the air-ingress rate is controlled by molecular diffusion through this opening.

Validation of the air-ingress mitigation method was conducted by CFD methods. The results show that both methods are effectively mitigating air-ingress process.

ACKNOWLEDGMENTS

This work was supported through the Department of Energy's NGNP Project under DOE Idaho Operations Office Contract DE-AC07-99ID13727.

REFERENCES

ANSYS, 2008, ICEM CFD-11.0, Manual.

NO, H.C., H. S. Lim, J. Kim, C. H. Oh, L. Siefken, and C. Davis, 2007, "Multi-component diffusion analysis and assessment of GAMMA code and improved RELAP 5 code," *Nuclear Engineering and Design*, Vol. 237, pp. 997–1008.

Ogawa, M, 1993, "Mass Transfer with Graphite Oxidation in Gas Mixture Laminar Flow through Circular Tube," *J. At. Energy Soc. Jpn.*, Vol. 35, Issue 3, p. 245.

Oh, C. H., C. Davis, L. Siefken, R. Moore, H. C. NO, J. Kim, G. C. Park, J. C. Lee, and W. R. Martin, 2006, *Development of Safety Analysis Codes and Experimental Validation for a Very High Temperature Gas-Cooled Reactor, Final Report*, INL/EXT-06-01362, Idaho National Laboratory, March 2006.

Oh, C. H., E. S. Kim, H. C. NO, and N. Z. Cho, 2008, *Experimental Validation of Stratified Flow Phenomena, Graphite Oxidation, and Mitigation Strategies of Air Ingress Accident, FY 2008 Report,* INL/EXT-08-14840, Idaho National Laboratory, December 2008.

Oh, C. H., E. S. Kim, S. Kang Hyung, H. C. NO, and N. Z. Cho, 2009, *Experimental Validation of Stratified Flow Phenomena, Graphite Oxidation, and Mitigation Strategies of Air Ingress Accident, FY 2008 Report*, INL/EXT-09-16465, Idaho National Laboratory, December 2009.

Schultz, R. R., et al., 2006, *Next Generation Nuclear Plant Methods Technical Program Plan*, INL/EXT-06-11804, September 2006.